Highly Oxidized Ruthenium Organometallic Compounds. The Synthesis and One-Electron Electrochemical Oxidation of [Cp*$Ru^{IV}Cl_2(S_2CR)$] (Cp* = η^5-C_5Me_5, R = NMe_2, NEt_2, O^iPr)

Seah Ling Kuan, Elaine Phuay Leng Tay, Weng Kee Leong, and Lai Yoong Goh*

Department of Chemistry, National University of Singapore, Kent Ridge, Singapore 117543

Ching Yeh Lin and Peter M. W. Gill

Research School of Chemistry, Australian National University, Canberra, ACT 0200, Australia

Richard D. Webster*

Division of Chemistry and Biological Chemistry, Nanyang Technological University, Singapore 637616

Received September 22, 2006

[Cp*$Ru^{IV}Cl_2(S_2CR)$] (R = NMe_2, NEt_2, and O^iPr) were synthesized by the reaction of [Cp*$Ru^{III}Cl_2]_2$ with $[RC(S)S]_2$. One-electron electrochemical oxidation of [Cp*$RuCl_2(S_2CR)$] produces paramagnetic [Cp*$RuCl_2(S_2CR)]^+$, which are stable in CH_2Cl_2 solution for at least several hours at 233 K. EPR experiments performed at 293 K show isotropic signals ($g \approx 2.035$) with clearly defined hyperfine coupling to ^{99}Ru and ^{101}Ru of 25 G and with peak-to-peak line widths of 15 G. At temperatures below 153 K, axial-shaped EPR spectra were obtained with *g*-values close to 2 (2.050−2.008) and narrow peak-to-peak line widths (15 G). Results from DFT calculations indicate that approximately 70% of the spin density in [Cp*$RuCl_2(S_2CNMe_2)]^+$ is located on the ruthenium, although there is an increase of only 0.06 in the positive charge of the metal ion as a result of the oxidation. The high spin density on Ru supports the assignment of a *formally* Ru(V) oxidation state, which is unprecedented in organometallic chemistry. Chemical oxidation of Cp*$Ru^{IV}Cl_2(S_2CNMe_2)$ with $NO(PF_6)$ in CH_3CN resulted in the isolation of [Cp*$Ru^{IV}(MeCN)_2(S_2CNMe_2)]^{+2}$ (**4**), while oxidation with $[(4\text{-Br-}C_6H_4)_3N](SbCl_6)$ in CH_2Cl_2 resulted in the formation of chloro-bridged dimeric $[Cp^*Ru^{IV}Cl(S_2CNMe_2)]_2^{+2}$ (**5**). When **5** is dissolved in CD_3CN/CH_3CN, it immediately converts to **4**. Cyclic voltammetric experiments confirmed that in both solvents the chemical oxidation process occurred through the [Cp*$Ru^{V}Cl_2(S_2CNMe_2)]^+$ intermediate.

1. Introduction

Transition metal complexes containing sulfur donor ligands command a continuing interest on account of their relevance to biological and industrial processes.[1] The dithiocarbamate (dtc) ligand has attracted particular attention as a versatile ligand in both main group[2a] and transition metal[2b] chemistry. A notable feature of dithiocarbamate ligands is their ability to stabilize metal species in high or unusual oxidation states,[3a] such as $[Co^{IV}(S_2CNR_2)_3]^+$ (R = alkyl or cyclohexyl), which is stable in CH_2Cl_2 at 233 K.[3b] In this study we report the synthesis of new (η^5-C_5Me_5)Ru(IV) complexes containing dithiocarbamate and carbonodithiolate ligands, which are able to be oxidized by one electron to form paramagnetic species, and discuss the distribution of the increased positive charge and spin density based on results from EPR spectroscopic experiments and DFT calculations.

Ru-containing dithiocarbamate compounds have recently been comprehensively reviewed,[2b] and there exists a number of complexes where the dithiocarbamate ligand has been coordinated together with the organometallic η^5-cyclopentadienyl ligand.[4] The electrochemical behavior of dithiocarbamate complexes has also been extensively studied.[3] One interesting case involves the oxidation of $[Ru^{III}(S_2CNR_2)_3]$, which was expected to form $[Ru^{IV}(S_2CNR_2)_3]^+$ on the basis of the observation that the related $[Fe^{IV}(S_2CNR_2)_3]^+$ (and Mn(IV)) complexes were

* Corresponding authors. E-mail: chmgohly@nus.edu.sg. Fax: +65 67791691. E-mail: webster@ntu.edu.sg, Fax: +65 67911961.

(1) See, for instance, the following and the references therein: (a) Dubois, M. R. *Chem. Rev.* **1989**, *89*, 1−9. (b) Holm, R. H.; Ciurli, S.; Weigel, J. A. *Prog. Inorg. Chem.* **1990**, *38*, 1−74. (c) Shibahara, T. *Coord. Chem. Rev.* **1993**, *123*, 73−147. (d) Sánchez-Delgado, R. A. *J. Mol. Catal.* **1994**, *86*, 287−307. (e) *Transition Metal Sulfur Chemistry−Biological and Industrial Significance*; Stiefel, E. I., Matsumoto, K., Eds.; ACS Symposium Series 653; American Chemical Society: Washington, DC, 1996. (f) Howard, J. B.; Rees, D. C. *Chem. Rev.* **1996**, *96*, 2965−2982. (g) Burgess, B. K.; Lowe, D. J. *Chem. Rev.* **1996**, *96*, 2983−3011. (h) Sellman, D.; Sutter, J. *Acc. Chem. Res.* **1997**, *30*, 460−469. (i) Curtis, M. D.; Druker, S. H. *J. Am. Chem. Soc.* **1997**, *119*, 1027−1036. (j) Mathur, P. *Adv. Organomet. Chem.* **1997**, *41*, 243−314. (k) Bianchini, C.; Meli, A. *Acc. Chem. Res.* **1998**, *31*, 109−116. (l) Ogino, H.; Inomata, S.; Tobita, H. *Chem. Rev.* **1998**, *98*, 2093−2121.

(2) (a) Heard, P. J. In *Progress In Inorganic Chemistry*; Karlin, K. D., Ed.; Wiley: New Jersey, 2005; Vol. 53, Chapter 1. (b) Hogarth, G. In *Progress in Inorganic Chemistry*; Karlin, K. D., Ed.; Wiley: New Jersey, 2005; Vol. 53, Chapter 2.

(3) (a) Bond, A. M.; Martin, R. L. *Coord. Chem. Rev.* **1984**, *54*, 23−98. (b) Webster, R. D.; Heath, G. A.; Bond, A. M. *J. Chem. Soc., Dalton Trans.* **2001**, 3189−3195, and references therein.

(4) (a) Wilczewski, T.; Bochenska, M.; Biernat, J. F. *J. Organomet. Chem.* **1981**, *215*, 87−96. (b) Wilczewski, T. *J. Organomet. Chem.* **1981**, *224*, C1−C4. (c) Reventos, L. B.; Alonso, A. G. *J. Organomet. Chem.* **1986**, *309*, 179−185. (d) Rao, K. M.; Mishra, L.; Agarwala, U. C. *Polyhedron* **1987**, *6*, 1383−1390. (e) Cordes, A. W.; Draganjac, M. *Acta Crystallogr. Sect. C* **1988**, *44*, 363−364. (f) McCubbin, Q. J.; Stoddart, F. J.; Welton, T.; White, A. J. P.; Williams, D. J. *Inorg. Chem.* **1998**, *37*, 3753−3758. (g) Coto, A.; Tenorio, M. J.; Puerta, M. C.; Valerga, P. *Organometallics* **1998**, *17*, 4392−4399. (h) Dodo, N.; Matsushima, Y.; Uno, M.; Onitsuka, K, Takahashi, S. *J. Chem. Soc., Dalton Trans.* **2000**, 35−41. (i) Kovács, I.; Lebuis, A.-M.; Shaver, A. *Organometallics* **2001**, *20*, 35−41. (j) Hogarth, G.; Faulkner, S. *Inorg. Chim. Acta* **2006**, *359*, 1018−1022.

10.1021/om060866z CCC: $33.50
Publication on Web 11/16/2006

stable.[5] Instead, one-electron oxidation of $[Ru^{III}(S_2CNR_2)_3]$ produced dimeric $[Ru_2^{III}(S_2CNR_2)_5]^+$ complexes.[6] Interestingly, the seven-coordinate $[Ru^{IV}Cl(S_2CNR_2)_3]$ and $[Ru^{IV}Cl(S_2CNR_2)_2(\eta^2\text{-}SCNR_2)]$ complexes were obtained by photolysis of $[Ru^{III}(S_2CNR_2)_3]$, suggesting that chloride aids in stabilizing the Ru(IV) state.[7] Dithiocarbamate complexes of ruthenium invariably exist between the oxidation states of II to IV,[4] which is similar to what is most often observed for organometallic compounds, although the concept of formal oxidation state does not adequately describe the true charge on the metal.[8] Nevertheless, the observation of a one-electron oxidation of a formally Ru(IV) organometallic compound is an interesting and surprising result worthy of detailed investigation.

2. Experimental Section

2.1. Electrochemical Procedures. Voltammetric experiments were conducted with a computer-controlled Eco Chemie μAutolab III potentiostat using planar 1 mm diameter Pt and glassy carbon (GC) working electrodes in conjunction with a Pt auxiliary electrode and an Ag wire reference electrode connected to the test solution via a salt bridge containing 0.5 M Bu_4NPF_6 in CH_3CN. Accurate potentials were obtained using ferrocene as an internal standard. In situ UV−vis−NIR spectra were obtained with a Varian Cary 5E spectrophotometer in an optically transparent thin-layer electrochemical (OTTLE) cell (path length = 0.05 cm) at 253 K using a Pt mesh working electrode.[3b,9] Typical exhaustive electrolysis time for the one-electron oxidation of 1 mM analyte in CH_2Cl_2 (0.5 M Bu_4NPF_6) was 1.5 h.

Solutions of $[Cp^*RuCl_2(S_2CR)]^+$ for the EPR experiments were prepared in a divided controlled potential electrolysis cell separated with a porosity no. 5 (1.0−1.7 μm) sintered glass frit.[3b,10] The working and auxiliary electrodes were identically sized Pt mesh plates symmetrically arranged with respect to each other with an Ag wire reference electrode (isolated by a salt bridge) positioned to within 2 mm of the surface of the working electrode. The electrolysis cell was jacketed in a glass sleeve and cooled to 233 K using a Lauda RL6 variable-temperature methanol-circulating bath. The volumes of both the working and auxiliary electrode compartments were approximately 10 mL each. The number of electrons transferred during the bulk oxidation process was calculated from

$$N = Q/nF \quad (1)$$

where N = no. of moles of starting compound, Q = charge (coulombs), n = no. of electrons, and F is the Faraday constant (96 485 C mol^{-1}). The electrolyzed solutions were transferred under vacuum into a cylindrical 3 mm (i.d.) EPR tube that was immediately frozen in liquid N_2 or to a silica flat cell that was cooled in dry ice/ethanol. EPR spectra were recorded on either a Bruker ER 200D (for T = 133−293 K with liquid N_2 cooling) or Bruker ESP 300e (for T = 6 K with liquid He cooling). Both spectrometers employed rectangular TE_{102} cavities with the modulation frequency set at 50−100 kHz and microwave power between 20 μW and 20 mW. EPR simulations were performed using the Bruker computer software WINEPR SimFonia. Other general procedures were as previously described.[10b−f]

2.2. Synthetic Procedures. Synthesis of $[Cp^*RuCl_2(S_2CNMe_2)]$ (1). To an orange-red solution of $[Cp^*RuCl_2]_2$ (1.25 g, 2.04 mmol) in acetonitrile (10 mL) was added $[Me_2NC(S)S]_2$ (0.49 g, 2.04 mmol) with stirring. The solution turned purple instantly. The resultant solution was filtered through a disk (2 cm) of silica gel. Concentration of the filtrate in vacuo to ca. 3 mL, followed by addition of ether (5 mL) and subsequent cooling at −30 °C for 30 min gave a microcrystalline dark purple solid of **1** (1.51 g, 3.53 mmol, 87%). Anal. Found: C, 36.1; H, 4.85; N, 3.2; S, 14.4; Cl, 17.0. Calcd for $C_{13}H_{21}Cl_2N_1Ru_1S_2$: C, 36.5; H, 4.95; N, 3.3; S, 15.0; Cl, 16.6. ^{1}H NMR (δ, $CDCl_3$): 1.42 (s, 15H, Me_5C_5), 3.31 (s, 6H, 2CH_3); (δ, CD_3CN): 1.32 (s, 15H, Me_5C_5), 3.27 (s, 6H, 2 CH_3). ^{13}C{^{1}H} NMR (δ, $CDCl_3$): 8.3 (Me_5C_5), 37.0 (CH_3), 106.4 (Me_5C_5), 205.9 (CS). IR (KBr, cm^{-1}): ν(C−N) 1566vs; ν(C−S) 1072 m, 1020 m. FAB$^+$ MS: m/z 392 ([M − Cl]$^+$), 357 ([M − 2 Cl]$^+$), 324 ([M − 2 Cl− 2 Me]$^+$).

Similar reactions of $[Cp^*RuCl_2]_2$ with $[Et_2NC(S)S]_2$ and $[^iPrOC(S)S]_2$ gave microcrystalline solids of $Cp^*RuCl_2(S_2CNEt_2)$ (**2**) and $Cp^*RuCl_2(S_2CO^iPr)$ (**3**), respectively. Full synthetic and characterization details will be described in a different context in a forthcoming paper.

Oxidation of $[Cp^*RuCl_2(S_2CNMe_2)]$ (1). (i) With $NO(PF_6)$. To a stirred purple solution of **1** (25 mg, 0.06 mmol) in ca. 5 mL of MeCN was added $NO(PF_6)$ (10 mg, 0.06 mmol, 1 molar equiv). The solution turned from purple to red instantly. After 5 min, the resultant solution was concentrated to ca. 2 mL and ether (3 mL) added. Subsequent cooling at −30 °C for 30 min gave a microcrystalline solid of **1** (11 mg, 0.03 mmol, 44% recovery). The mother liquor was concentrated to ca. 2 mL, followed by addition of ether (ca. 3 mL), and subsequent cooling at −30 °C for a day afforded a red microcrystalline solid of $[Cp^*Ru(MeCN)_2(S_2CNMe_2)](PF_6)_2$ (**4**) (7 mg, 0.01 mmol, 16%), leaving a residual red oil, which showed the presence of only complex **4** in its ^{1}H NMR spectrum. Anal. Found: C, 27.7; H, 3.9; N, 5.3; S, 8.9. Calcd for $C_{17}H_{27}F_{12}N_3P_2Ru_1S_2$: C, 28.0; H, 3.7; N, 5.8; S, 8.8. ^{1}H NMR (δ, CD_3CN): 1.49 (s, 15H, Me_5C_5), 1.95 (s, CH_3CN, overlapping with solvent peak), 3.29 (s, 6H, 2CH_3). ^{13}C{^{1}H} NMR (δ, CD_3CN): 8.93 (Me_5C_5), 38.6 (CH_3),114.1 (Me_5C_5), 200.7 (CS). IR (KBr, cm^{-1}): ν(C≡N) 2322 w 2297 w; ν(C−N) 1580 m; ν(C−S) 1082 w 1019 m. FAB$^+$ MS: m/z 356 [M − 2MeCN]$^+$. FAB$^-$ MS: m/z 145 [PF_6]. ESI$^+$ MS: m/z 397 [M − MeCN]$^+$ 356 [M − 2MeCN]$^+$. ESI$^+$ MS: m/z 145 [PF_6].

A repeat of the reaction of **1** (43 mg, 0.10 mmol), with 2 molar equiv of $NO(PF_6)$ (35 mg, 0.20 mmol), followed by a similar workup, gave a microcrystalline solid of **4** (36 mg, 0.05 mmol, 49.4%) and a red mother liquor that showed the presence of only complex **4** in its ^{1}H NMR spectrum.

The reaction of **1** (21 mg, 0.05 mmol) with 2 molar equiv of $NO(PF_6)$ (18 mg, 0.10 mmol) was repeated in 10 mL of dichloromethane at 0 °C. The purple color of the solution gradually assumed a reddish tinge after 20 min and then finally turned green after a further 10 min. Upon evacuation to dryness, a green oil was obtained. No attempt was made to characterize the green oil.

(5) (a) Pasek, E. A.; Straub, D. K. *Inorg. Chem.* **1972**, *11*, 259−263. (b) Golding, R. M.; Harris, C. M.; Jessop, K. H.; Tennant, W. C. *Aust. J. Chem.* **1972**, *25*, 2567−2576.

(6) Mattson, B. M.; Heiman, J. R.; Pignolet, L. H. *Inorg. Chem.* **1976**, *15*, 564−571.

(7) (a) Given, K. W.; Mattson, B. M.; Pignolet, L. H. *Inorg. Chem.* **1976**, *15*, 3152−3156. (b) Miessler, G. L.; Pignolet, L. H. *Inorg. Chem.* **1979**, *18*, 210−213.

(8) Bennett, M. A.; Khan, K.; Wenger, E. In *Comprehensive Organometallic Chemistry II*; Abel, E. W., Stone, F. G. A., Wilkinson, G., Shriver, D. F., Bruce, M. I., Eds.; Pergamon: Oxford, 1995; Vol. 7, Chapter 8.

(9) (a) Webster, R. D.; Heath, G. A. *Phys. Chem. Chem. Phys.* **2001**, *3*, 2588−2594. (b) Arnold, D. P.; Hartnell, R. D.; Heath, G. A.; Newby, L.; Webster, R. D. *J. Chem. Soc., Chem. Commun.* **2002**, 754−755. (c) Williams, L. L.; Webster, R. D. *J. Am. Chem. Soc.* **2004**, *126*, 12441−12450.

(10) (a) Webster, R. D. *Magn. Reson. Chem.* **2000**, *38*, 897−906. (b) Shin, R. Y. C.; Ng, S. Y.; Tan, G. K.; Koh, L. L.; Khoo, S. B.; Goh, L. Y.; Webster, R. D. *Organometallics* **2004**, *23*, 547−558. (c) Shin, R. Y. C.; Tan, G. K.; Koh, L. L.; Goh, L. Y.; Webster, R. D. *Organometallics* **2004**, *23*, 6108−6115. (d) Shin, R. Y. C.; Tan, G. K.; Koh, L. L.; Vittal, J. J.; Goh, L. Y.; Webster, R. D. *Organometallics* **2005**, *24*, 539−551. (e) Shin, R. Y. C.; Teo, M. E.; Leong, W. K.; Vittal, J. J.; Yip, J. H. K.; Goh, L. Y.; Webster, R. D. *Organometallics* **2005**, *24*, 1483−1494. (f) Kuan, S. L.; Leong, W. K.; Goh, L. Y.; Webster, R. D. *Organometallics* **2005**, *24*, 4639−4648.

Table 1. Crystallographic Data Collection and Processing Parameters

	1	4	5
formula	$C_{13}H_{21}Cl_2NRuS_2$	$C_{21}H_{33}F_{12}N_5P_2RuS_2$	$C_{13}H_{21}Cl_7NRuS_2Sb$
M_r	427.4	810.65	726.40
temp, K	223(2)	223(2)	223(2)
cryst color and habit	black block	red plate	red plate
cryst size, mm	0.07 × 0.08 × 0.18	0.28 × 0.20 × 0.06	0.48 × 0.36 × 0.02
cryst syst	orthorhombic	orthorhombic	monoclinic
space group	$P2_12_12_1$	$P2_12_12_1$	$P2_1/n$
a, Å	8.6825(5)	9.3012(4)	8.2628(5)
b, Å	11.6053(7)	12.2982(5)	11.0759(7)
c, Å	17.1190(10)	28.5968(13)	26.4815(16)
α, deg	90	90	90
β, deg	90	90	96.5860(10)
γ, deg	90	90	90
V, Å^3	1724.96(18)	3271.1(2)	2407.5(3)
Z	4	4	4
density, Mg m^{-3}	1.646	1.646	2.004
abs coeff, mm^{-1}	1.447	0.795	2.700
F(000)	864	1632	1408
θ range for data collection	2.12 to 30.84	1.80 to 27.49	2.40 to 26.37
index ranges	$-12 \le h \le 12$, $0 \le k \le 16$, $0 \le l \le 24$	$-12 \le h \le 9$, $15 \le k \le 15$, $-37 \le l \le 36$	$-10 \le h \le 10$, $0 \le k \le 13$, $0 \le l \le 33$
no. of reflns collected	13 792	23 277	19 829
no. of indep reflns	4998 [R(int) = 0.075]	7472 [R(int) = 0.0487]	4928 [R(int) = 0/0513]
no. of data/restraints/params	4998/0/179	7472/0/399	4928/0/233
final R indices [$I > 2\sigma(I)$][a,b]	R1 = 0.0444, wR2 = 0.0688	R1 = 0.0520, wR2 = 0.1153	R1 = 0.0893, wR2 = 0.1903
R indices (all data)	R1 = 0.0631, wR2 = 0.0734	R1 = 0.0589, wR2 = 0.1186	R1 = 0.0969, wR2 = 0.1940
goodness-of-fit on F^2[c]	0.869	1.097	1.315
largest diff peak and hole, e Å^{-3}	1.883 and −0.743	1.044 and −0.734	2.483 and −1.844

[a] $R = (\sum||F_o| - |F_c||)\sum|F_o|$. [b] $wR2 = [(\sum w|F_o| - |F_c|)^2/\sum w|F_o|^2]^{1/2}$. [c] $GoF = [(\sum w|F_o| - |F_c|)^2/(N_{obs} - N_{param})]^{1/2}$.

(ii) With [(4-Br-C$_6$H$_4$)$_3$N](SbCl$_6$). Ten milliliters of dichloromethane was added to a mixture of **1** (21 mg, 0.05 mmol) and [(4-Br-C$_6$H$_4$)$_3$N](SbCl$_6$) (41 mg, 0.05 mmol), with stirring. Red solids slowly precipitated out of the dark blue solution after ca. 30 min. The mixture was allowed to stir overnight; the supernatant was then light blue. The product mixture was filtered, and the red solid of [Cp*RuCl(S$_2$CNMe$_2$)]$_2$(SbCl$_6$)$_2$ (**5**) (20 mg, 0.03 mmol, 55.0%) was washed with diethyl ether (3 × 5 mL) and collected. Anal. Found: C, 21.1; H, 2.9; N, 1.9; S, 8.5. Calcd for $C_{26}H_{42}Cl_{14}N_2Ru_2S_4Sb_2$: C, 21.5; H, 2.9; N, 1.9; S, 8.8. IR (KBr, cm^{-1}): ν(C−N) 1561 s 1543.2 m; ν(C−S) 1042 w 1020 m. Complex **5** was initially sparingly soluble in deuterated MeCN, but dissolved completely after ultrasonication for ca. 20 min to give a light red solution. The ^{1}H NMR spectrum of this solution indicated the presence of complex **4**, while that of the blue supernatant indicated the presence of the starting material, **1**, which was not recovered.

2.3. X-ray Diffraction Studies. Diffraction-quality single crystals were obtained at −30 °C as follows: **1** as dark purple crystals from an acetonitrile solution layered with ether after 2 days, **4** as red plates from an acetonitrile solution layered with ether after a day, and **5** as red plates by slow diffusion of layers of precooled solutions of [(4-Br-C$_6$H$_4$)$_3$N](SbCl$_6$) (10 mg in 2 mL in dichloroethane) and **1** (5 mg in 1 mL in dichloromethane) over 2−3 days.

The crystals were mounted on glass fibers. X-ray data were collected on a Bruker APEX AXS diffractometer, equipped with a CCD detector, using Mo Kα radiation (λ 0.71073 Å). The program SMART[11a] was used for collecting frames of data, indexing reflection, and determination of lattice parameter, SAINT[11b] for integration of the intensity of reflections, scaling, and correction of Lorentz and polarization effects, SADABS[11c] for absorption correction, and SHELXTL[11d] for space group and structure determination and least-squares refinements on F^2. The structures of **1**, **4**, and **5** were solved by direct methods to locate the heavy atoms, followed by difference maps for the light non-hydrogen atoms. The crystal data collection and processing parameters are given in Table 1.

2.4. Theoretical Calculations. Density functional theory (DFT) calculations were performed using the Q-Chem 3.0 software package,[12] and molecular structures were optimized using the B3LYP functional.[13] The 3-21G basis set was used for all atoms except Ru, for which the SRSC basis and pseudopotential[14] were employed. The exchange−correlation quadrature used the SG-0 grid[15] on all atoms except Ru, for which the larger SG-1 grid[16] was used. Natural bond orbital (NBO) analysis of atomic charges and spin densities were obtained from orbitals computed using the B3LYP functional; for these calculations, a large, all-electron basis containing 90 basis functions[17] was used for Ru, the STO-3G basis for H atoms, and the 6-31G* basis for all other atoms. To compute spin densities at the nuclei, it is common to sample the density using a delta function operator. However, because this can lead to inaccurate results when used with Gaussian basis sets, we have employed the Rassolov−Chipman operator and the range parameter $r_0 = 0.25$ au.[18]

(11) (a) *SMART* version 5.628; Bruker AXS Inc.: Madison, WI, 2001. (b) *SAINT+* version 6.22a; Bruker AXS Inc.: Madison, WI, 2001. (c) Sheldrick, G. M. *SADABS*; 1996. (d) *SHELXTL* version 5.1; Bruker AXS Inc.: Madison, WI, 1997.

(12) Shao, Y.; Fusti-Molnar, L.; Jung, Y.; Kussmann, J.; Ochsenfeld, C.; Brown, S. T.; Gilbert, A. T. B.; Slipchenko, L. V.; Levchenko, S. V.; O'Neill, D. P.; DiStasio, R. A.; Lochan, R. C.; Wang, T.; Beran, G. J. O.; Besley, N. A.; Herbert, J. M.; Lin, C. Y.; van Voorhis, T.; Chien, S. H.; Sodt, A.; Steele, R. P.; Rassolov, V. A.; Maslen, P. E.; Korambath, P. P.; Adamson, R. D.; Austin, B.; Baker, J.; Byrd, E. F. C.; Daschel, H.; Doerksen, R. J.; Dreuw, A.; Dunietz, B. D.; Dutoi, A. D.; Furlani, T. R.; Gwaltney, S. R.; Heyden, A.; Hirata, S.; Hsu, C. P.; Kedziora, G.; Khalliulin, R. Z.; Klunzinger, P.; Lee, A. M.; Lee, M. S.; Liang, W. Z.; Lotan, I. Nair, N.; Peters, B.; Proynov, E. I.; Pieniazek, P. A.; Rhee, Y. M.; Ritchie, J.; Rosta, E.; Sherrill, C. D.; Simmonett, A. C.; Subotnik, J. E.; Woodcock, H. L.; Zhang, W.; Bell, A. T.; Chakraborty, A. K.; Chipman, D. M.; Keil, F. J.; Warshel, A.; Hehre, W. J.; Schaefer, H. F.; Kong, J.; Krylov, A. I.; Gill, P. M. W.; Head-Gordon, M. *Phys. Chem. Chem. Phys.* **2006**, *8*, 3172−3191.

(13) Stephens, P. J.; Devlin, F. J.; Chabalowski, C. F.; Frisch, M. J. *J. Phys. Chem.* **1994**, *98*, 11623−11627.

(14) Andrae, D.; Haussermann, U.; Dolg, M.; Stoll, H.; Preuss, H. *Theor. Chim. Acta* **1990**, *77*, 123−141.

(15) Chien, S. H.; Gill, P. M. W. *J. Comput. Chem.* **2006**, *27*, 730−739.

(16) Gill, P. M. W.; Johnson, B. J.; Pople, J. A. *Chem. Phys. Lett.* **1993**, *209*, 506−512.

(17) *Handbook of Gaussian Basis Sets*; Poirier, R., Kari, R., Csizmadia, I. G., Eds.; Elsevier: New York, 1995.

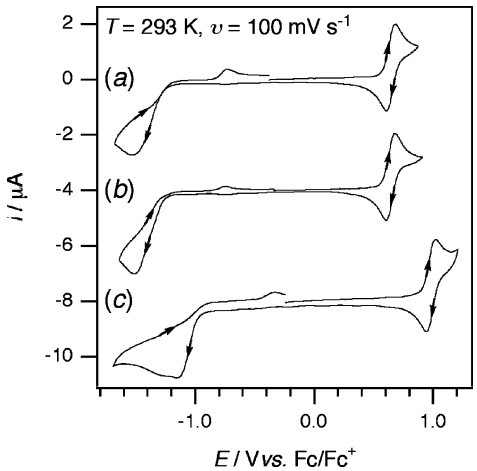

Figure 1. Cyclic voltammograms recorded in CH_2Cl_2 with 0.5 M Bu_4NPF_6 at a Pt electrode of 1.0 mM solutions of (a) [Cp*$RuCl_2(S_2CNMe_2)$], **1**, (b) [Cp*$RuCl_2(S_2CNEt_2)$], **2**, and (c) [Cp*$RuCl_2(S_2CO^iPr_2)$], **3**. (b) and (c) are offset by -4 and -8 μA, respectively.

Scheme 1

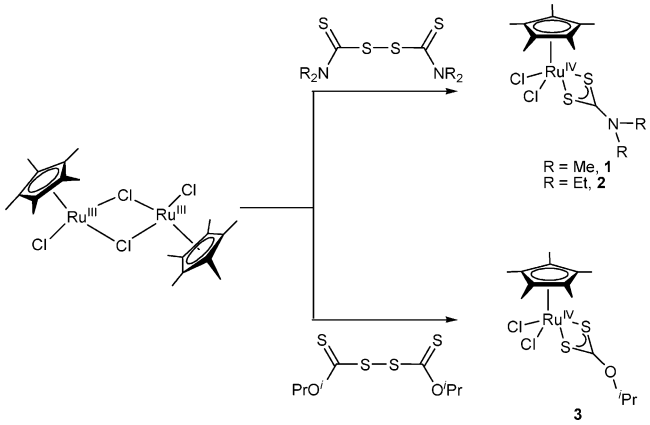

3. Results and Discussion

The Ru(IV) complexes [Cp*$RuCl_2(S_2CR)$] (**1**, R = NMe_2; **2**, R = NEt_2; **3**, R = O^iPr) were obtained in high yields from the reaction of $[Cp^*Ru^{III}Cl_2]_2$ with $[RC(S)S]_2$ (Scheme 1).

Cyclic voltammograms of CH_2Cl_2 solutions containing [Cp*$RuCl_2(S_2CR)$] showed complicated reduction processes at negative potentials that varied depending on the electrode surface and temperature (Figure 1). The presence of electrochemical reduction responses is certainly the expected result considering the high oxidation state of Ru(IV) and the rich literature pertaining to low oxidation state η^5-(Cp/Cp*)Ru compounds.[8] However, considerably more surprising was the observation of oxidation processes at $E^r_{1/2} = +0.65$ V vs Fc/Fc^+ (Fc = ferrocene) (for [Cp*$RuCl_2(S_2CNMe_2)$] **1** and [Cp*$RuCl_2(S_2CNEt_2)$] **2**) and $E^r_{1/2} = +0.98$ V vs Fc/Fc^+ (for [Cp*$RuCl_2(S_2CO^iPr)$] **3**), suggesting the formation of highly oxidized ruthenium organometallic compounds.[19] In contrast to the reduction processes, the oxidation processes appeared fully chemically reversible at temperatures between 233 and 293 K with anodic (i_p^{ox}) to cathodic (i_p^{red}) peak-to-peak separations similar to those observed for Fc under identical conditions, and with i_p^{ox}-values proportional to $\upsilon^{1/2}$ (υ = scan rate). Furthermore, exhaustive bulk electrochemical oxidation at a potential 0.1 V more positive than the i_p^{ox}-values resulted in the transfer of 1.0 $\pm$ 0.1 electrons per molecule, with the oxidized compounds stable enough (at $T = 233$ K) to be reduced back to the starting material when the applied potential was switched to $\lesssim +0.5$ V vs Fc/Fc^+. While compounds containing the dithiocarbamate ligand are known to undergo dimerization following oxidation (or other ligand-based reactions),[3] the chemically reversible nature of the voltammetric process on the short (CV) and long (electrolysis) time scales confirms the straightforward one-electron oxidation of [Cp*$RuCl_2(S_2R)$] to form [Cp*$RuCl_2(S_2R)]^+$ (the counteranion for all experiments was the supporting electrolyte anion, PF_6^-).

There is little uncertainty that ruthenium is present as formally Ru(IV) in the neutral diamagnetic starting material (each ligand carries a charge of -1), but the formal oxidation state of Ru in the one-electron-oxidized form is ambiguous when based solely on electrochemical experiments, especially considering that Ru(V) is unprecedented in organometallic chemistry and rarely observed in coordination chemistry.[20] However, the alternative possibility where the oxidation is entirely ligand-based is also unlikely since neither the dithiocarbamate or Cp* ligands are strong candidates for a localized one-electron oxidation. Nevertheless, the strong dependence of $E^r_{1/2}$ (that approximates the formal potential, E^0) on the dithiocarbamate or carbonodithiolate groups indicates that the bidentate sulfur ligands are critically involved in the oxidation process.

Samples of [Cp*$RuCl_2(S_2R)]^+$ for EPR spectroscopic analysis were prepared by one-electron oxidation of the starting material in an electrolysis cell and then transferred under vacuum into silica EPR cells. The X-band EPR spectra of [Cp*$RuCl_2(S_2CNMe_2)]^+$ at 293 K showed an intense symmetrical ($S = {}^1/_2$) signal with a g-value of 2.035 and a peak-to-peak line width (ΔH_{pp}) of 15 G. The solution phase spectra also showed the presence of weaker satellite signals symmetrically arranged on either side of the main signal (Figure 2a). The presence of satellite signals of weaker intensity than the primary signal is an indication of hyperfine interactions with lower abundance isotopes. The intensity and pattern of the satellite signals are in excellent agreement with hyperfine coupling (of 25 G) to ^{99}Ru ($I = {}^5/_2$, 12.72% natural abundance) and ^{101}Ru ($I = {}^5/_2$, 17.07% natural abundance) (see simulation in Figure 2a), indicating an interaction of the unpaired electron with the metal ion.

The intensity of the $^{99}Ru/^{101}Ru$ hyperfine coupling on either side of the main $S = {}^1/_2$ signal became increasingly less symmetrical as the temperature was lowered from 293 to 193 K, possibly due to an anisotropic tumbling effect (Figure 2b).[21] At temperatures below $\sim$193 K (when the solution began to freeze) the spectra were axial shaped ($g_\perp = 2.050$, $g_\parallel = 2.008$) and remained constant in appearance down to 6 K. The line width of the spectra also remained constant (15 G) over the entire temperature range (293$-$6 K), suggesting that the oxidized compound maintains the same geometric structure in solution and frozen solution states. The EPR signal began to diminish in intensity if the sample was left at 293 K for over 30 min, but at low temperatures ($T < 233$ K) the compound appeared stable for at least several hours. Very similar EPR spectra were detected for [Cp*$RuCl_2(S_2CNEt_2)]^+$ and [Cp*$RuCl_2(S_2CO^iPr)]^+$ (Figure 2c), with $^{99}Ru/^{101}Ru$ hyperfine coupling values also

(18) (a) Rassolov, V. A.; Chipman, D. M. *J. Chem. Phys.* **1996**, *105*, 1470$-$1478. (b) Rassolov, V. A.; Chipman, D. M. *J. Chem. Phys.* **1996**, *105*, 1479$-$1491.

(19) The reversible half-wave potential, $E^r_{1/2} = (E_p^{ox} + E_p^{red})/2$, where E_p^{ox} and E_p^{red} are the anodic and cathodic peak potentials, respectively.

(20) Che, C.-M.; Lau, T.-C. In *Comprehensive Coordination Chemistry II*; McCleverty, J. A., Meyer, T. J., Constable, E. C., Dilworth, J. R., Eds.; Elsevier: Oxford, 2004; Vol. 5, pp 800$-$809.

(21) Weil, J. A.; Bolton, J. R.; Wertz, J. E. In *Electron Paramagentic Resonance: Elementary Theory and Practical Applications*; Wiley: New York, 1994; pp 320$-$327.

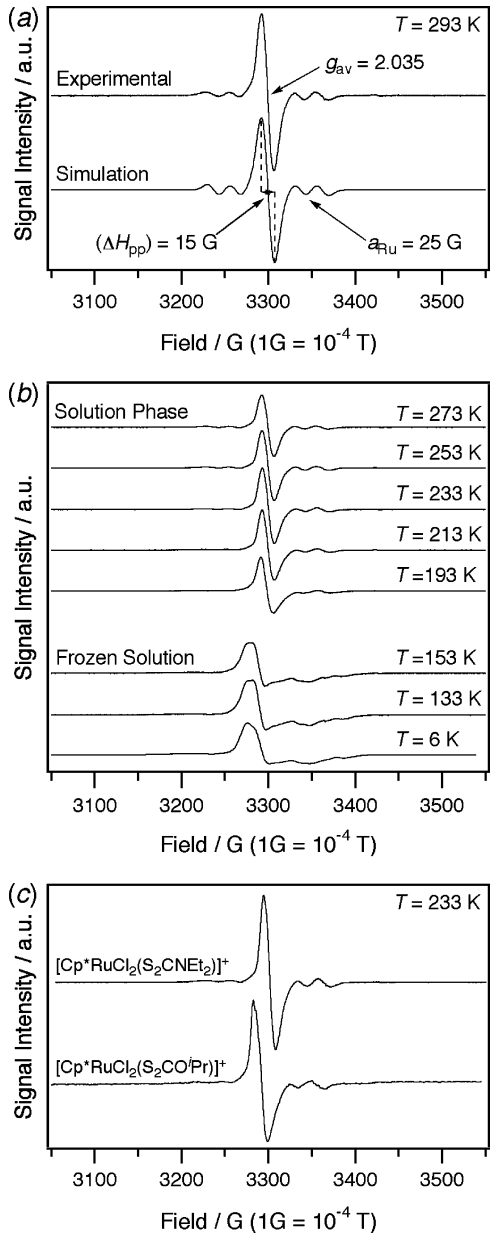

Figure 2. First derivative continuous wave X-band EPR spectra recorded in CH_2Cl_2 with 0.5 M Bu_4NPF_6: (a) $[Cp^*RuCl_2(S_2CNMe_2)]^+$, $\mathbf{1}^+$, at 293 K; (b) $[Cp^*RuCl_2(S_2CNMe_2)]^+$, $\mathbf{1}^+$, between 273 and 6 K; (c) $[Cp^*RuCl_2(S_2CNEt_2)]^+$, $\mathbf{2}^+$, and $[Cp^*RuCl_2(S_2CO^iPr)]^+$, $\mathbf{3}^+$, at 233 K.

equal to 25 G. $[Cp^*RuCl_2(S_2CO^iPr)]^+$ was not stable at temperatures above 233 K, possibly because its higher oxidation potential increased its reactivity.

Discussion on the EPR spectra of d^5 Ru(III) coordination and organometallic compounds is usually restricted to *g* matrix components,[22] although Ru anisotropic hyperfine interactions are sometimes observed at low temperatures with hyperfine coupling of approximately 50 G.[23] EPR spectra of complexes containing formally Ru(V) ions are scarce. A sharp single-line isotropic EPR signal (without any hyperfine structure) was detected for $(n\text{Pr}_4\text{N})[\text{Ru}^{\text{V}}(\text{O})(\text{O}_2\text{COCEt}_2)_2]$ at room temperature.[24] Most of the reports of hyperfine coupling in Ru

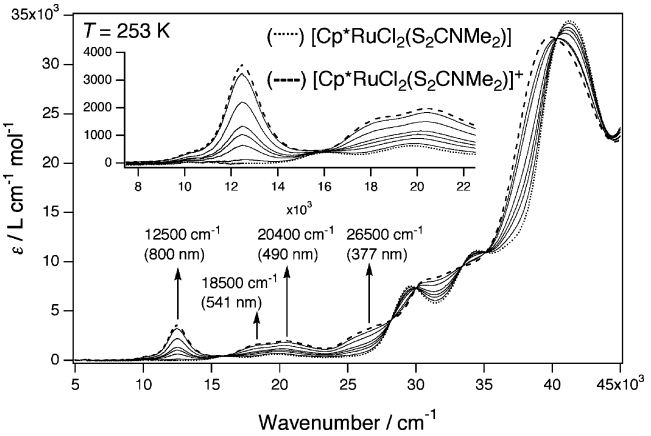

Figure 3. UV−vis−NIR spectra obtained during the one-electron in situ electrochemical oxidation of 1.0 mM $[Cp^*RuCl_2(S_2CNMe_2)]$, **1**, in CH_2Cl_2 with 0.5 M Bu_4NPF_6 in an OTTLE cell.

compounds involve ligand-centered radicals coordinated to Ru(II) ions and with hyperfine coupling constants < 10 G.[25,26] Therefore, the 25 G Ru hyperfine coupling found in this work is significantly larger than observed for ligand-centered radicals and suggests that the oxidized compounds contain Ru in the most highly oxidized state recorded in organometallic chemistry. Hyperfine coupling to other nuclei in the complexes such as Cl, N, or H is possible. However, because of the relatively narrow line width of the spectrum, any additional hyperfine coupling can be estimated to be very small (<3−4 G) in order not to complicate the spectra in Figure 3. This indicates that most of the unpaired electron spin density must be located within the region of the Ru ion.

DFT calculations using the B3LYP functional were performed on $[Cp^*RuCl_2(S_2CMe_2)]$ and its one-electron-oxidized form to complement the experimental EPR studies, in order to locate the increased positive charge and unpaired electron spin density (Table 2). The calculations predict an increase of only 0.06 in the positive charge on the metal ion as a result of the oxidation, with the remaining increase in positive charge shared mainly between the Cp* group (0.37), the chlorides (0.30), and the sulfurs (0.15). However, although the DFT calculations predict a relatively small increase in positive charge of the metal ion in the oxidized compound, they predict that the majority of the unpaired electron spin density (70%) is located on the metal ion, thereby leading to the important conclusion that the oxidized compound does have a metal-centered spin state. DFT calculations of the spin density at each nucleus in the oxidized compound reveal that this is an order of magnitude higher for Ru (−0.2) than for any other nucleus (Table 2), although there

(22) Rieger, P. H. *Coord. Chem. Rev.* **1994**, *135/136*, 203−286.
(23) (a) Pruchnik, F. P.; Galdecka, E.; Galdecki, Z.; Kowalski, A. *Polyhedron* **1999**, *18*, 2091−2097. (b) Gugger, P. A.; Willis, A. C.; Wild, S. B.; Heath, G. A.; Webster, R. D.; Nelson, J. H. *J. Organomet. Chem.* **2002**, *643*−*644*, 136−153.
(24) Dengel, A. C.; Griffith, W. P. *Inorg. Chem.* **1991**, *30*, 869−871.
(25) (a) Kaim, W.; Kohlmann, S. E. S.; Welkerling, P. *Chem. Phys. Lett.* **1985**, *118*, 431−434. (b) Poppe, J.; Moscherosch, M.; Kaim, W. *Inorg. Chem.* **1993**, *32*, 2640−2643. (c) Waldhör, E.; Schwederski, B.; Kaim, W. *J. Chem. Soc., Perkin Trans. 2* **1993**, 2109−2111. (d) Krejcik, M.; Zalis, S.; Klima, J.; Sykora, D.; Matheis, W.; Klein, A.; Kaim, W. *Inorg. Chem.* **1993**, *32*, 3362−3368. (e) Waldhör, E.; Poppe, J.; Kaim, W.; Cutin, E. H.; García, Posse, M. E.; Katz, N. E. *Inorg. Chem.* **1995**, *34*, 3093−3096. (f) Ye, S.; Sarkar, B.; Duboc, C.; Fiedler, J.; Kaim, W. *Inorg. Chem.* **2005**, *44*, 2843−2847.
(26) (a) Sherlock, S. J.; Boyd, D. C.; Moaser, B.; Gladfelter, W. L. *Inorg. Chem.* **1991**, *30*, 3626−3632. (b) Sun, Y.; DeArmond, M. K. *Inorg. Chem.* **1994**, *33*, 2004−2008. (c) Samuels, A. C.; DeArmond, M. K. *Inorg. Chem.* **1995**, *34*, 5548−5551. (d) Araújo, C. S.; Drew, M. G. B.; Félix, V.; Jack, L.; Madureira, J.; Newell, M.; Roche, S.; Santos, T. M.; Thomas, J. A.; Yellowlees, L. *Inorg. Chem.* **2002**, *41*, 2250−2259. (e) Chanda, N.; Paul, D.; Kar, S.; Mobin, S. M.; Datta, A.; Puranik, V. G.; Rao, K. K.; Lahiri, G. K. *Inorg. Chem.* **2005**, *44*, 3499−3511.

Table 2. Calculated[a] Atomic Charges, Spin Densities, and Spin Densities at the Nuclei in the Neutral and Oxidized Forms of [Cp*RuCl$_2$(S$_2$CNMe$_2$)] (1)

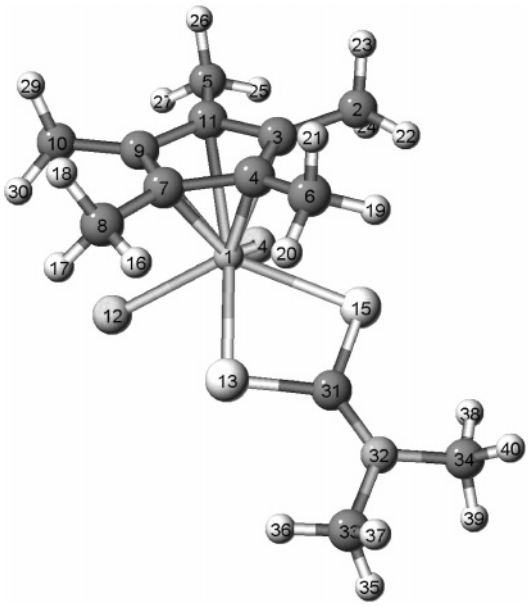

		charge			spin density	spin density at nucleus
atom no.	atom type	[Cp*RuCl$_2$(S$_2$CNMe$_2$)]	[Cp*RuCl$_2$(S$_2$CNMe$_2$)]$^+$	[Cp*RuCl$_2$(S$_2$CNMe$_2$)]$^+$–[Cp*RuCl$_2$(S$_2$CNMe$_2$)]	[Cp*RuCl$_2$(S$_2$CNMe$_2$)]$^+$	[Cp*RuCl$_2$(S$_2$CNMe$_2$)]$^+$
1	Ru	0.38	0.44	0.06	0.69	−0.21
2	C	−0.70	−0.70	0	0	0
3	C	−0.03	0.01	0.03	0	0
4	C	−0.03	0.01	0.03	0	0
5	C	−0.70	−0.70	0	0	0
6	C	−0.69	−0.70	0	0	0
7	C	−0.03	0.01	0.03	0	0
8	C	−0.70	−0.70	0	0	0
9	C	0	0.04	0.04	0.01	0.01
10	C	−0.70	−0.70	0	0	0
11	C	0	0.04	0.04	0.01	0.01
12	Cl	−0.45	−0.30	0.15	0.12	0.02
13	S	0.03	0.11	0.08	0	0
14	Cl	−0.45	−0.30	0.15	0.12	0.02
15	S	0.03	0.11	0.08	0	0
16	H	0.26	0.27	0.01	0	0
17	H	0.27	0.28	0.01	0	0
18	H	0.26	0.28	0.02	0	0
19	H	0.26	0.27	0.01	0	0
20	H	0.26	0.27	0.01	0	0
21	H	0.26	0.28	0.02	0	0
22	H	0.26	0.27	0.01	0	0
23	H	0.26	0.28	0.02	0	0
24	H	0.27	0.28	0.01	0	0
25	H	0.27	0.28	0.01	0	0
26	H	0.26	0.28	0.02	0	0
27	H	0.27	0.28	0.01	0	0
28	H	0.27	0.28	0.01	0	0
29	H	0.26	0.28	0.02	0	0
30	H	0.27	0.28	0.01	0	0
31	C	−0.06	−0.05	0.01	0	0
32	N	−0.42	−0.38	0.04	0.04	0.01
33	C	−0.48	−0.47	0	0	0
34	C	−0.48	−0.47	0	0	0
35	H	0.24	0.26	0.02	0	0
36	H	0.26	0.26	0	0	0
37	H	0.24	0.26	0.02	0	0
38	H	0.26	0.26	0	0	0
39	H	0.24	0.26	0.02	0	0
40	H	0.24	0.26	0.02	0	0

[a] Optimized structures and natural bond orbital analysis using the B3LYP functional. See text for basis set and Rassolov−Chipman details.

is also a significant contribution to spin density within the outer d-orbitals of the Ru.

Further evidence for the spin density on the metal in the one-electron-oxidized compound came from UV−vis−NIR experiments. The spectrum of the starting material showed only two weak bands below 25 000 cm^{-1}, at 16 000 and ∼20 000 cm^{-1}, that are likely to be associated with d−d transitions due to their low intensity ($\epsilon \approx 500$ L cm^{-1} mol^{-1}).[27] The higher intensity ($\epsilon \approx 10\,000$ L cm^{-1} mol^{-1}) bands in the starting material at ∼30 000 and 35 000 cm^{-1} are ligand-to-metal charge transfer (LMCT) excitations,[27] while the highest intensity band, at ∼40 000 cm^{-1} ($\epsilon \approx 35000$ L cm^{-1} mol^{-1}), results from $\pi-\pi^*$ transitions in the dithiocarbamate ligand.[3b] The UV−vis−NIR spectra of [Cp*RuCl$_2$(S$_2$CNMe$_2$)]$^+$ showed a series of bands

Scheme 2

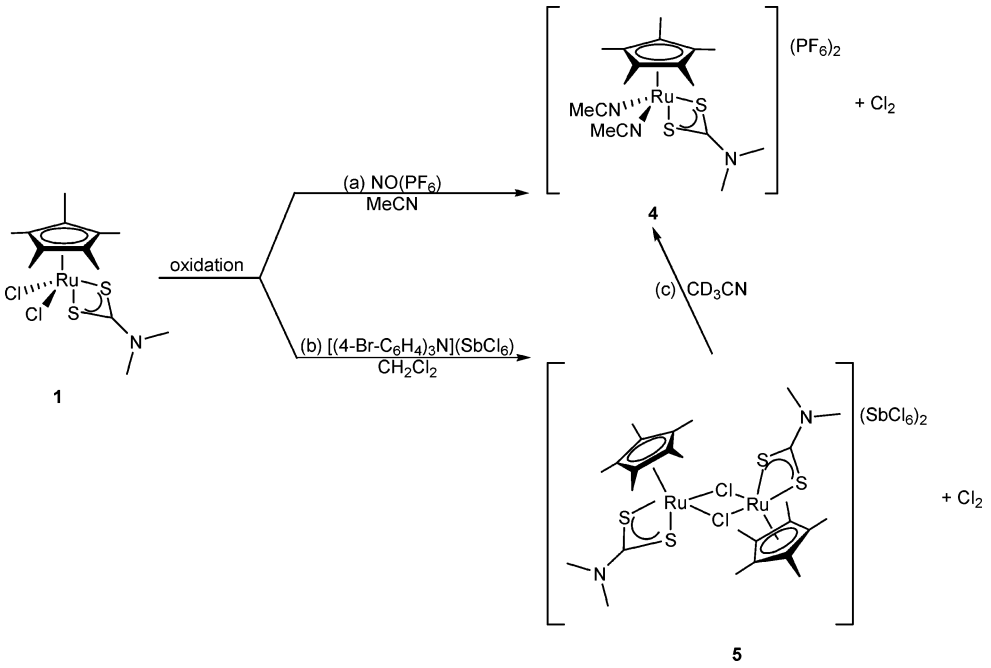

at $\nu = 12\,500$, 18 500, 20 400, and 26 500 cm^{-1}, which, due to their intensity ($\epsilon = 2000-4000$ L cm^{-1} mol^{-1}), can be interpreted as LMCT excitations (and are likely to obscure any new d−d transitions).[3b,27] The presence of new bands ($\nu <$ 30 000 cm^{-1}) in the spectrum of the oxidized compound can be rationalized by an electronic state that facilitates low-energy LMCT transitions to the partially filled metal orbital. A similar result was observed during the oxidation of $[Co^{III}(S_2CNEt_2)_3]$ to $[Co^{IV}(S_2CNEt_2)^3]^+$ (a d^6 to d^5 change).[3b]

The in situ electrochemical UV−vis−NIR spectra obtained during the one-electron oxidation of $[Cp^*Ru^{IV}Cl_2(S_2CNMe_2)]$ at 253 K were completely reversible, so that applying a potential sufficiently negative to cause the reduction of $[Cp^*RuCl_2(S_2CNMe_2)]^+$ resulted in the regeneration of the spectrum with the same appearance and signal intensity as the starting material (Figure 3). The stability of $[Cp^*RuCl_2(S_2CNMe_2)]^+$ on the time frame of the experiment (2−3 h) was also supported by the occurrence of several isosbestic points at 15 800, 28 200, 30 000, 33 400, 35 100, and 40 300 cm^{-1}.

Chemical Oxidation of $[Cp^*RuCl_2(S_2CNMe_2)]$ (1). Attempts were made to isolate $[Cp^*RuCl_2(S_2CNMe_2)]^+$ detected in the electrochemical studies on complex **1**, by performing a one-electron chemical oxidation. $[Cp^*RuCl_2(S_2CNMe_2)]$ (**1**) is oxidized at $E^r_{1/2} = +0.65$ V vs Fc/Fc^+ (Fc = ferrocene); hence $NO(PF_6)$, a known one-electron oxidant, with an $E° = +0.70$ V vs Fc/Fc^+ (Fc = ferrocene) in acetonitrile[28] was chosen for this purpose. Upon addition of 1 equiv of $NO(PF_6)$ to a purple solution of complex **1**, the color of the solution turned red instantaneously. From this red solution, another Ru(IV) species, $[Cp^*Ru(MeCN)_2(S_2CNMe)](PF_6)_2$ (**4**), was isolated, in which two of the chloro ligands have been substituted by acetonitrile molecules (Scheme 2a). Cyclic voltammetry experiments performed on **1** in acetonitrile at $\upsilon = 100$ mV s^{-1} indicated that **1** could be oxidized in a one-electron chemically reversible process to $\mathbf{1}^+$ (i.e., the same as in CH_2Cl_2). However, longer term CPE and in situ electrochemical UV−vis experiments in CH_3CN indicated that $\mathbf{1}^+$ decomposed/reacted within 1 h of forming; therefore, the cation was less stable in CH_3CN than in CH_2Cl_2.

Scheme 3

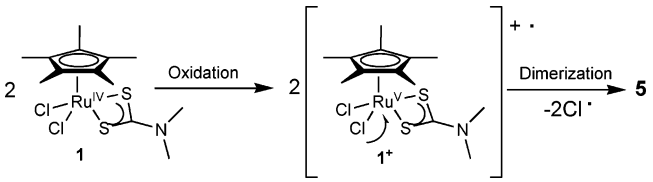

Chemical oxidation experiments were also performed with $NO(PF_6)$ in CH_2Cl_2, but the one-electron-oxidized product did not appear stable in this medium in the presence of NO^+ or $NO_{(g)}$. Another attempt was made to synthesize the Ru(V) complex using the one-electron oxidant $[(4\text{-}Br\text{-}C_6H_4)_3N](SbCl_6)$.[28] The reaction in dichloromethane led to slow precipitation within 30 min of red solids of **5**, the X-ray structure of which showed a dichloro-bridged dimeric Ru(IV) species, $[Cp^*Ru(S_2CNMe_2)]_2(SbCl_6)_2$, in agreement with microanalytical data (Scheme 2b). The red solid of **5** was initially insoluble in CD_3CN; however, ultrasonication for 20 min gave a light red solution. The ^1H NMR spectrum of this solution matched that of complex **4** (less the proton signals of coordinated MeCN), indicating that the polar coordinating acetonitrile facilitated dissociation of the dimer, with concomitant or subsequent ligand displacement (Scheme 2c). It is likely that oxidation in acetonitrile also progresses through the dimeric compound **5** (such a process readily explains the charge balance), but MeCN quickly reacts to form the monomeric coordinated compound, **4**.

Electrochemical experiments proved that **1** was indeed oxidized to $\mathbf{1}^+$ in both CH_2Cl_2 and MeCN; thus the instability of $\mathbf{1}^+$ over synthetic time scales is likely to be due to the highly oxidizing nature of Ru(V). The consequence is secondary oxidation of the chloride ligands (Scheme 3), with concomitant reduction of the Ru(V) to Ru(IV), as found in **4** in a coordinating solvent and **5** in a noncoordinating solvent. This postulation is in agreement with DFT calculation on the Ru(V) species, $[Cp^*RuCl_2(S_2CNMe_2)]^+$, which predicted that most of the increased positive charge is located on the Cl atoms (although *not* the unpaired electron spin density). Such reactions where

(27) Lever, A. B. P. In *Inorganic Electronic Spectroscopy*, 2nd ed.; Elsevier: Amsterdam, 1984.

(28) Connelly, N. G.; Geiger, W. E. *Chem. Rev.* **1996**, *96*, 877−910.

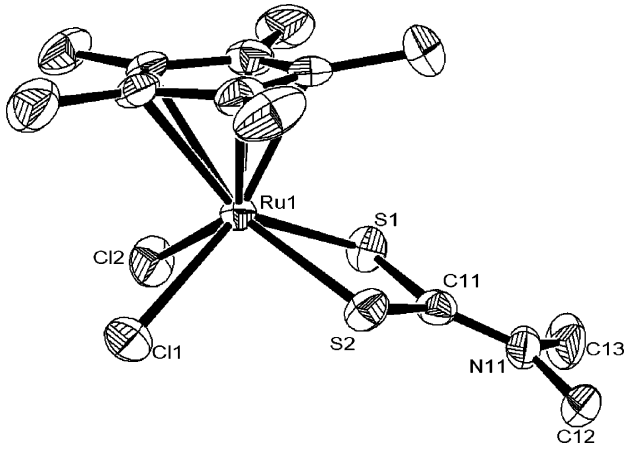

Figure 4. ORTEP plot for the molecular structure of [Cp*$RuCl_2(S_2CNMe_2)$], **1** (a selected view that omits the disorder in Cp*). Thermal ellipsoids are drawn at the 50% probability level, and hydrogen atoms are omitted for clarity. Selected bond lengths (Å) and angles (deg): Ru(1)−S(1) 2.3706(12), Ru(1)−S(2) 2.3681(10), S(1)−C(11) 1.712(5), S(2)−C(11) 1.724(4), N(11)−C(11) 1.304(5), S(2)−Ru(1)−S(1) 71.16(4), S(1)−C(11)−S(2) 106.7(2).

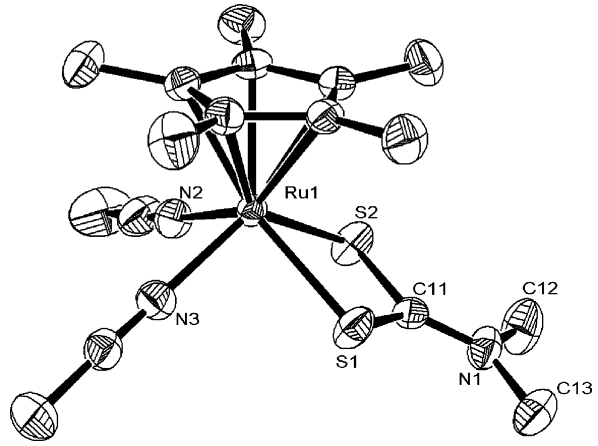

Figure 5. ORTEP plot for the molecular structure of [Cp*Ru$(MeCN)_2(S_2CNMe_2)]^{2+}$, **4** (a selected view that omits the PF_6 anions and solvent of crystallization). Thermal ellipsoids are drawn at the 50% probability level, and hydrogen atoms are omitted for clarity. Selected bond lengths (Å) and angles (deg): Ru(1)−S(1) 2.3906(13), Ru(1)−S(2) 2.3798 (14), S(1)−C(11) 1.704(5), S(2)−C(11) 1.715(5), N(1)−C(11) 1.304(6), S(2)−Ru(1)−S(1) 70.64(5), S(1)−C(11)−S(2) 107.5(3).

the ligands are oxidized by the metal in high oxidation states are not unknown; for instance, Bond and co-workers had previously reported intheir study of reactivity of Ir^{IV} dithiocarbamates (dtc) and diselenocarbamates (dsc) complexes in solution that $[Ir(Et_2dsc)_3]^+$ slowly dimerizes during the course of bulk electrolysis experiments and subsequently undergoes an internal redox reaction to give $[Ir_2(Et_2dsc)_5]^+$ and oxidized ligand.[29] The authors also reported that the $[Ir(dtc)_3]^+$ cations are highly oxidizing in nature, as is demonstrated by their oxidation of free dithiocarbamate ion to give thiuram disulfide and by the oxidation of elemental mercury to give mixed-metal complexes $[HgIr_2(dtc)_6]^{2+}$. The possibility that complexes **4** and **5** are formed via direct oxidation of the chloride ligands in the [Cp*$RuCl_2(S_2CNMe_2)$] starting material is not supported by the electrochemical, UV−vis, and EPR spectroscopic experiments that prove the existence of $\mathbf{1}^+$.

Crystallography. The molecular structures of complexes **1**, **4**, and **5** are shown in Figures 4, 5, and 6, with selected bond lengths and bond angles. In all three instances, the Cp*Ru complexes adopt a four-legged piano stool configuration, with the dtc ligand occupying two coordination sites and the remaining two sites taken by chloride (in **1** and **5**) or acetonitrile (in **4**). The structure of $\mathbf{5}^+$ possesses a center of inversion in the Ru(1)−Cl(1)−Ru(1A)−Cl(1A) plane.

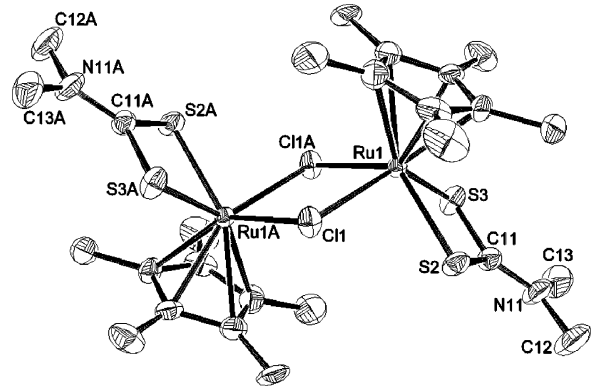

Figure 6. ORTEP plot for the molecular structure of [Cp*RuCl$(S_2CNMe_2)]_2^{2+}$, **5** (a selected view that omits the $SbCl_6$ anions). Thermal ellipsoids are drawn at the 50% probability level, and hydrogen atoms are omitted for clarity. Selected bond lengths (Å) and angles (deg): Ru(1)−S(2) 2.367 (3), Ru(1)−S(3) 2.364(3), Ru(1)−Cl(1) 2.424(3), Ru(1)−Cl(1A) 2.447(2), S(2)−C(11) 1.712(10), S(3)−C(11) 1.697(10), N(11)−C(11) 1.309(13), S(2)−Ru(1)−S(3) 70.88(10), S(2)−C(11)−S(3) 107.2(5), Ru(1)−Cl(1)−Ru(1A) 101.21(9).

4. Conclusions

$[Cp^*RuCl_2(S_2CNMe_2)]^+$ contains Ru in possibly the most highly oxidized state ever recorded in organometallic chemistry. Electrochemical, EPR, and UV−vis spectroscopic studies indicate that in CH_2Cl_2 the oxidized compound ($\mathbf{1}^+$) is stable for at least several hours at 233 K, but on preparative time scales reacts to form a dimeric compound (**5**) via loss of $Cl^\bullet$. **5** reacts readily with 4 equiv of MeCN to form **4**, the monomeric analogue of **1** containing 2 MeCN ligands. The assignment of a formally Ru(V) state in ($\mathbf{1}^+$) is based on EPR experiments that detected hyperfine coupling to $^{99/101}$Ru and from density-based calculations that predicted 70% unpaired electron spin density on the Ru. The high spin density on Ru is in contrast to the calculated small increase (0.06) in positive charge on Ru following oxidation.

Acknowledgment. The authors thank NUS for financial support (ARF grant nos. R143000-135 and 209-112 to L.Y.G., and graduate research scholarships to S.L.K. and E.P.L.T.) and the ARC for the award of a QEII Fellowship (R.D.W.). We also thank Prof. M. A. Bennett and Dr. R. Bramley of the Research School of Chemistry, ANU, for helpful discussions on organometallic chemistry and EPR spectroscopy, respectively, and Dr. L. L. Koh and Ms. G. K. Tan for technical assistance.

Supporting Information Available: Full X-ray crystallographic data in CIF format relating to the collection and refinement of complexes **1**, **4**, and **5**. This material is available free of charge via the Internet at http://pubs.acs.org.

OM060866Z

(29) Bond, M. A.; Colton, R.; Mann, D. R. *Inorg. Chem.* **1990**, *29*, 4665−4611.